Experimental evidence for an intermediate phase in the multiferroic $YMnO_3$

2007 J. Phys.: Condens. Matter 19 466212

(http://iopscience.iop.org/0953-8984/19/46/466212)

IOP PUBLISHING JOURNAL OF PHYSICS: CONDENSED MATTER

J. Phys.: Condens. Matter **19** (2007) 466212 (9pp) doi:10.1088/0953-8984/19/46/466212

Experimental evidence for an intermediate phase in the multiferroic $YMnO_3$

G Nénert[1], M Pollet[2], S Marinel[3], G R Blake[1], A Meetsma[1] and T T M Palstra[1]

[1] Solid State Chemistry Laboratory, Zernike Institute for Advanced Materials, University of Groningen, Nijenborg 4, 9747 AG Groningen, The Netherlands
[2] ICMCB-CNRS Physico-Chimie des Oxides Conducteurs, 87 Avenue du Docteur Schweitzer 33608 Pessac Cedex, France
[3] Laboratoire CRISMAT, UMR CNRS ENSI Caen-14050, Caen Cedex 4, France

Received 24 April 2007, in final form 22 August 2007
Published 25 October 2007
Online at stacks.iop.org/JPhysCM/19/466212

Abstract

We have studied $YMnO_3$ by high-temperature synchrotron x-ray powder diffraction, and have carried out differential thermal analysis and dilatometry on a single crystal sample. These experiments show two phase transitions at about 1100 K and 1350 K, respectively. This demonstrates the existence of an intermediate phase between the room temperature ferroelectric and the high-temperature centrosymmetric phase. This study identifies for the first time the different high-temperature phase transitions in $YMnO_3$.

1. Introduction

In typical ferroelectrics the creation of an electric dipole moment involves a charge transfer between empty d-shell metal ions and occupied 2p orbitals of oxygen. This mechanism of ferroelectricity precludes magnetic moments and magnetic order. $YMnO_3$ is part of a class of materials that exhibit both electric and magnetic orders, called multiferroics. The coexistence of ferroelectricity and magnetic order allows the manipulation of electric and magnetic moments by magnetic and electric fields, respectively [1]. In multiferroics, the charge transfer from the 2p orbitals towards the transition metal ion is not relevant due to the partially filled nature of the d-shell. Indeed, in $YMnO_3$ the Mn-ion remains in the barycenter of its oxygen coordination. However, this charge transfer is allowed towards the empty d-shell of the rare-earth and creates two dipoles of opposite sign, resulting in a ferrielectric state[4]. Recent *ab initio* calculations indicate that the ferrielectric state involves no charge transfer, but is related to the tilting of the

[4] The structure of $YMnO_3$ can be described by layers of edge-sharing trigonal bipyramids of oxygen surrounding Mn atoms. These layers are separated by layers of Y. The rare-earth atoms have a non-conventional seven-fold coordination. A cooperative buckling of the MnO_5 trigonal bipyramids below T_{FE} displaces the Y^{3+} ions along the c axis. The displacements of the two symmetrically inequivalent Y ions in the unit cell are in opposite directions. Thus we call the polarized state of $YMnO_3$ a ferrielectric state (two opposite non-compensated polarizations).

MnO_5 polyhedra [2]. However, there is no clear high-temperature structural information about this transition to clarify the origin of the ferrielectric state in this material. While a lot of effort is put into the search and design of new multiferroics, the nature of the mechanism of ferrielectricity and thus the nature of the coupling between the different degrees of freedom is still not well understood in $YMnO_3$. We can distinguish two classes of antiferromagnetic ferroelectrics: T_N (Néel temperature) $> T_{FE}$ (critical temperature for ferroelectricity) and $T_N < T_{FE}$. For the first class, with compounds like RMn_2O_5 and o-$RMnO_3$ (orthorhombic), the mechanism of ferroelectricity can be understood phenomenologically by the existence of a gradient of the magnetization (incommensurate helicoidal spin structure) leading to a transverse polarization [3, 4]. The coexistence and strong coupling between ferroelectricity and incommensurate magnetism in o-$RMnO_3$ is related to Dzyaloshinskii–Moriya interactions [5]. For the second class, which includes h-$RMnO_3$ (hexagonal), the origin of ferroelectricity is not well understood since the Mn off-centering is not responsible for the ferroelectricity [2]. Moreover, the h-$RMnO_3$ is particularly interesting due the high polarization at room temperature ($P_S \sim 5.5\ \mu C\ cm^{-2}$). The h-$RMnO_3$ exhibit $T_{FE} \sim 1000$ K and $T_N \sim 100$ K. Despite this difference, recent studies of h-$RMnO_3$ show that the ferroelectric and antiferromagnetic order parameters are coupled [6–9].

$YMnO_3$ adopts the centrosymmetric space group $P6_3/mmc$ in its high-temperature paraelectric state and the polar space group $P6_3cm$ at room temperature with a unit cell that is tripled in volume (the a and b axes are lengthened by a factor of $\sqrt{3}$). However, the ferroelectric transition temperatures reported in the literature fall into two distinct groups, and when taken together, previous studies of $YMnO_3$ suggest that there are not one but two distinct phase transitions above room temperature [10]. However, these phase transitions have never both been observed in a single experiment. Moreover, it has consistently been reported that the ferroelectric transition of $YMnO_3$ occurs at 933 K and not higher as claimed by Abrahams *et al* [11]. If an intermediate phase (IP) exists, its symmetry and nature have not yet been determined.

In recent years, two structural studies have been carried out on h-$RMnO_3$ powder in the high-temperature regime either by synchrotron or by neutron diffraction [12, 13]. Both experiments failed to observe any structural phase transitions even though measurements were performed up to 1000 K for R = Y (synchrotron), up to 1300 K for R = Lu, 1100 K for R = Yb and 1400 K for R = Tm (neutron). Lonkai *et al* realized, using symmetry arguments, that two high-temperature phase transitions are necessary [13]. Therefore, they proposed an antiferroelectric IP having the same symmetry as the room temperature phase ($P6_3cm$). We believe that the absence of observations of phase transitions in these two recent studies, contradicting older results, has caused confusion regarding the high-temperature behavior of $YMnO_3$. The succession of three states has thus far been only theoretically incorporated into investigations of the origin of the ferroelectric state [2, 14]. The aim of this paper is to prove experimentally the existence of an IP in $YMnO_3$. Furthermore, we will show that our data are in agreement with previous experimental observations.

First, we report the room temperature structure of a high-quality single crystal. Using dilatometry and differential thermal analysis, we demonstrate in a single experiment the existence of an intermediate phase stable between T_{C1} and T_{C2}. In addition, based on synchrotron x-ray powder diffraction, we confirm the existence of the paraelectric phase above T_{C2} with the $P6_3/mmc$ symmetry. Finally, we discuss the differences in transition temperatures between our results and earlier reports in the light of single crystal quality.

2. Experimental techniques

$YMnO_3$ powder was synthesized by reacting stoichiometric amounts of Y_2O_3 (4N) and MnO_2 (3N metal basis) in nitrogen atmosphere at 1200 °C for 10 h. The powder was reground and

Table 1. Atomic coordinates of a single crystal $YMnO_3$ grown by the floating zone technique from data collected at room temperature. The cell parameters are $a = 6.1469(6)$ Å and $c = 11.437(1)$ Å (space group $P6_3cm$, $wR(F^2) = 8.45\%$ and $R(F) = 3.43\%$). In parentheses, we indicate the standard uncertainty. The z coordinate of Y_2 was fixed due to the lack of a center of symmetry.

Atoms	x	y	z	U_{eq} (Å^2)
Y_1	0	0	0.771 1(2)	0.0056(5)
Y_2	1/3	2/3	0.730 38(-)	0.0060(3)
Mn	0.6672(5)	0	0.497 6(2)	0.0059(5)
O_1	0.697(1)	0	0.661(1)	0.010(2)
O_2	0.353(1)	0	835 2(9)	0.005(2)
O_3	0	0	0.973(2)	0.008(3)
O_4	1/3	2/3	0.515(1)	0.010(3)

resintered once under the same conditions to improve crystallinity. A single crystal was grown from the powder in air by the Floating Zone technique using a four mirror furnace. The good crystallinity of the crystal was confirmed by Laue diffraction.

We have carried out an additional high-temperature synchrotron x-ray experiment on the beamline ID31 at ESRF (Grenoble, France) using a wavelength of 0.3 Å. The powder sample was placed in a spinning Pt capillary which was heated by means of a three mirror furnace. The temperature control was monitored by the position of the Pt peaks with a feedback system to compensate for the aging of the lamps. Rietveld refinements of the data were carried out using the GSAS software package [15].

In order to check the quality of our single crystal, we carried out a full data set collection at room temperature. A black crystal with approximate dimensions of 0.14 mm × 0.12 mm × 0.04 mm was measured at room temperature on a Bruker SMART APEX CCD diffractometer. Intensity measurements were performed using a graphite monochromatic Mo Kα radiation. The final unit cell was obtained from the xyz centroids of 1743 reflections after integration. Intensity data were corrected for Lorentz and polarization effects and for absorption [16]. The program suite SHELXTL was used for space group determination assuming an inversion twin [17].

The differential thermal analysis (DTA) was carried out in a flow of nitrogen using a SDT2960 of TA instruments between room temperature and 1473 K with a ramp of 5 K min^{-1}. We used a crushed single crystal for this experiment in a platinum pan.

The dilatometry measurements were carried out in static air using a SETARAM TMA92 dilatometer. The temperature ramp was 1 K min^{-1} starting from room temperature to 1473 K. A load of 10 g was applied on the single crystal to optimize the signal to noise ratio. The choice of this load was based on several trial runs. The sample used was cut in a rectangular shape, but not oriented along a particular crystallographic orientation. The single crystal was protected from the alumina parts using platinum sheets. All measurements were corrected for the blank signal (alumina + platinum).

3. Results and discussion

The refined atomic coordinates and isotropic displacement parameters of our crystal at room temperature are presented in table 1. The crystal contains inversion twins as a natural consequence of the polar structure. The structure is very similar to that previously reported [12]. However, there is a significant difference in the unit cell volume of our crystal compared

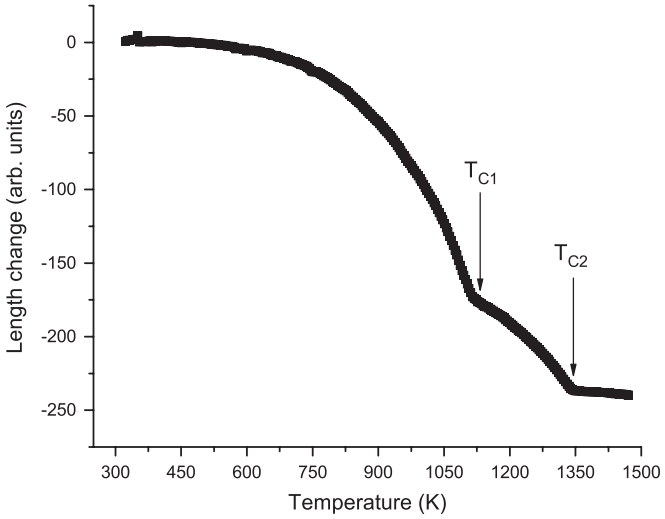

Figure 1. Dilatometry measurement of an unoriented single crystal of $YMnO_3$. The arrows indicate the two transition temperatures T_{C1} and T_{C2}.

Table 2. Comparison of the lattice parameters between single crystals grown from a Bi_2O_3 flux and this work.

Reference	a (Å)	c (Å)
[18]	6.145	11.42
[19]	6.1387(3)	11.4071(3)
[20]	6.125(1)	11.41(1)
This work	6.1469(6)	11.437(1)

with the structures of the single crystals grown from Bi_2O_3 flux (see table 2), even when experimental uncertainty is taken into account. We will discuss later the possible origin of such a difference and its consequence for the ferroelectric transition temperature.

In figure 1, we show the temperature dependence of the dilatometric response of an unoriented single crystal of $YMnO_3$. We observe clearly two anomalies while heating. The first anomaly, denoted T_{C1}, appears at about 1125 K and the second anomaly appears at $T_{C2} \sim 1350$ K. These transitions are also observed in our DTA experiment, shown in figure 3, where we notice anomalies at about 1100 K for T_{C1} and at ∼1350 K for T_{C2}.

We had a closer look at the temperature dependence of the thermomechanical analysis (TMA) response close to T_{C2}. In figure 2, we show a zoom of the TMA response close to T_{C2}, which is linear below about 1340 K. While measuring the TMA response, one measures the strain which usually plays the role of a secondary order parameter during a phase transition. Indeed, we know that the transition from the HT phase to the IP could involve some strain as a secondary order parameter [21]. The linear dependence on temperature of the TMA response suggests that the transition at T_{C2} is of second order.

In order to clarify the nature of the two phase transitions, we carried out a DTA experiment on a crushed single crystal under N_2 atmosphere. The results are presented in figure 3. We notice a small anomaly at T_{C1} and a larger one at T_{C2}. The differentiation between second order and first order phase transitions using DTA remains a non-straightforward task [22]. While we observe a large peak at about 1350 K, the DTA anomaly at about 1100 K is small. This suggests

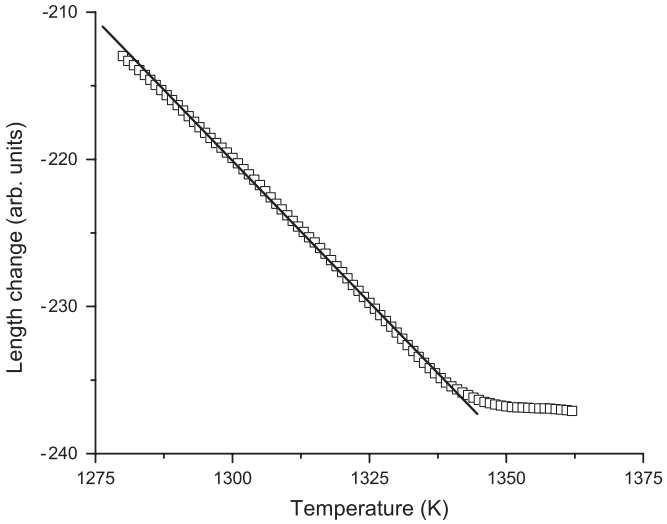

Figure 2. Linear temperature dependence below T_{C2} of the thermomechanical analysis.

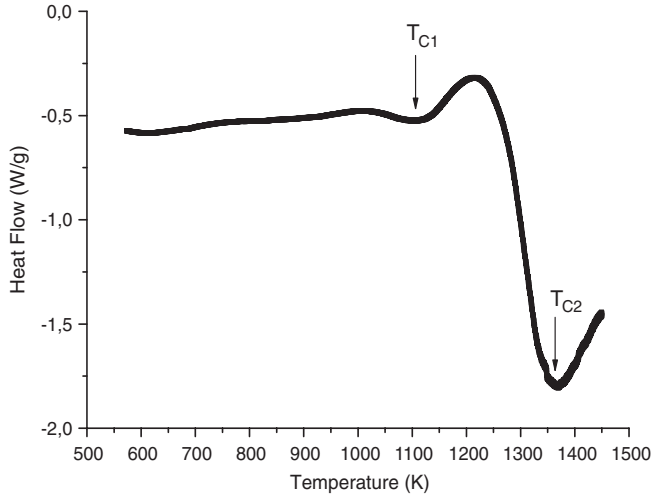

Figure 3. Differential thermal analysis of a crushed single crystal of $YMnO_3$. The measurement was carried out in a N_2 atmosphere with a rate of 5 K min^{-1}. The arrows indicate the ferroelectric transition temperature T_{C1} and the tripling of the unit cell T_{C2}.

that this transition at 1350 K requires significantly more energy than the one from IP towards the RT phase

We further investigated $YMnO_3$ using synchrotron x-ray powder diffraction. We collected data at several temperatures, concentrating on the range 950–1475 K. This is below and above the transition temperature T_{C2} observed in the dilatometry and DTA experiments. We present the measured cell parameters in figure 4.

In figure 4, we can clearly see an anomaly around 1350 K, characterizing the transition towards the high-temperature paraelectric phase with $P6_3/mmc$ symmetry [13, 18]. The transition at T_{C2} is confirmed by the disappearance of the (206) reflection, which is characteristic of the tripled unit cell, as shown in figure 5.

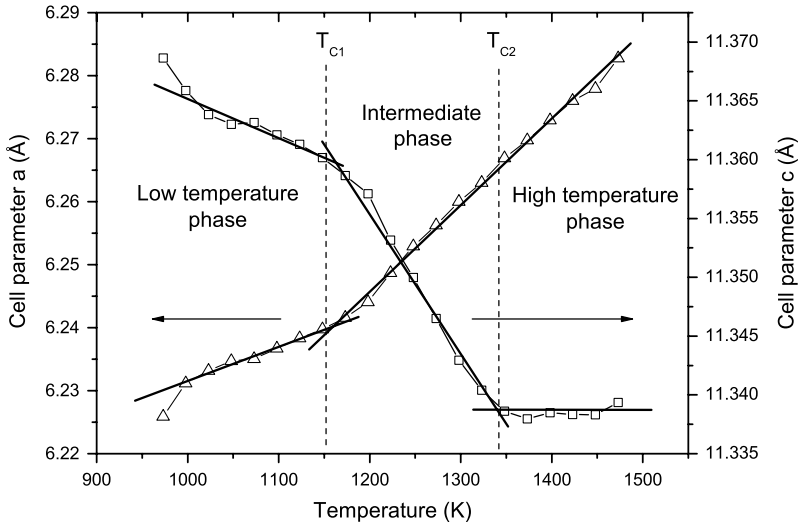

Figure 4. Cell parameters obtained from a powder sample at the ID31 beamline at ESRF with $P6_3cm$ symmetry. The high-temperature data above T_{C2} have the symmetry $P6_3/mmc$ and its cell parameters are $a' = \frac{a}{\sqrt{3}}$ and $c' = c$.

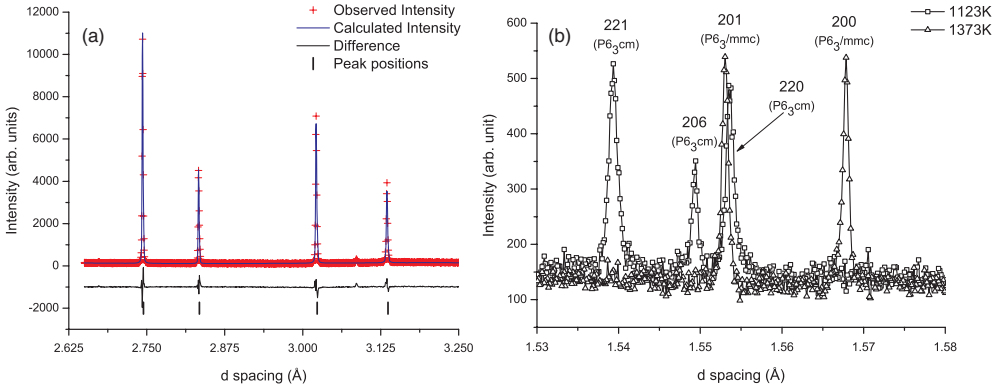

Figure 5. (a) Portion of the Rietveld refinement using the $P6_3/mmc$ symmetry at 1373 K, (b) disappearance of the (206) reflection as a function of temperature determined by x-ray synchrotron diffraction. This evidences the transition towards the $P6_3/mmc$ symmetry.

(This figure is in colour only in the electronic version)

We summarize in table 3 the atomic coordinates in the high-temperature centrosymmetric phase $P6_3/mmc$ at 1373 K. A physically meaningful model could be reached only by constraining all the U_{iso} of the different atoms to be equal.

We observe that the transition at T_{C2} in figure 4 does not show any discontinuity. Thus in the light of the results of dilatometry data, DTA and diffraction data, we interpret both transitions at T_{C1} and at T_{C2} as second order phase transitions. We notice that the transition at T_{C1} is more obvious in the dilatometry experiment than in the synchrotron x-ray powder data. We observe that the transition at T_{C1} in the powder sample appears to be broadened. This type of phenomenon is often seen in polycrystalline samples where different grains will undergo the transition at slightly different temperatures due to the effects of factors such as grain size,

Table 3. Atomic coordinates determined by x-ray synchrotron Rietveld refinement at 1373 K in the $P6_3/mmc$ symmetry. Cell parameters: $a = 3.621\,78(2)$ Å and $c = 11.3379(2)$ Å.

Atom	x	y	z	U_{iso}
Y	0	0	0	0.0270(7)
Mn	1/3	2/3	1/4	0.0270(7)
O_1	0	0	1/4	0.0270(7)
O_2	1/3	2/3	0.0821(8)	0.0270(7)

morphology and strain. Indeed a change in slope of the c cell parameter is seen in the vicinity of T_{C1} (see figure 4).

As we have already remarked, the unit cell for single crystals grown from a Bi_2O_3 flux is systematically smaller than for crystals grown by the floating zone technique. There are two possibilities to explain this difference: a significant amount of Bi could be incorporated in the structure and/or the number of vacancies can be different in the crystal structure caused by the different growth techniques.

We expect that if Bi is incorporated into the structure, it will preferentially occupy the seven-fold coordinated yttrium site. This hypothesis can be disregarded for several reasons. First, Bi^{3+} has a larger Shannon radius than Y^{3+}:$r(Bi^{3+}) = 1.24$ Å (derived from the average between six-fold coordination and eight-fold coordination) and $r(Y^{3+}) = 1.1$ Å [23]. Therefore, we expect an increase of the cell parameters. Second, we have carried out refinements of the occupation on both Y-sites using the dataset of van Aken *et al* [19] and our data. We did not find any evidence for substitution of Y by Bi. Thus, we have no experimental evidence for the incorporation of Bi into the lattice.

The second possible explanation for the smaller unit cell of flux-grown crystals is the creation of vacancies. According to Abrahams [24], vacancies would also affect the ferroelectric transition temperature, which can be expressed as (in kelvin):

$$T_{FE} = (\kappa/2k)(\Delta z)^2, \tag{1}$$

where κ is a force constant, k is Boltzmann's constant and Δz is the largest displacement along the polar c axis between the ferroelectric phase and the paraelectric phase. This value is expressed in Å due to $\Delta z = (z_{para} - z_{ferro}) \times c$. The ratio $\kappa/2k$ has been estimated as $2.00(9) \times 10^4$ K Å^{-2}. According to equation (1), a decrease of T_{FE} implies a decrease of the force constant, the displacement of the rare-earth z_{para}–z_{ferro} and/or the c lattice parameter. It is obvious that defects can be responsible for such changes. For instance, an excess in yttrium ($YMn_{1-x}O_{3-3/2x}$) would certainly both decrease the c parameter (consistent with the observations) and lower κ. In the same way, impurities can lower T_{FE}. Experiments using alumina crucibles instead of platinum can easily result in $YMn_{1-x}Al_xO_3$. Such a substitution would again account for a small decrease in the c parameter. All of these suggestions need to be checked experimentally. We note that the presence of oxygen vacancies within the structure is unlikely because they would lead to electrostatic repulsions between the cations, enlarging the unit cell.

The expected dependence of T_{C1} on the concentration of vacancies can explain the discrepancies between the recent results of Lonkai and Katsufuji and those in the older literature. Both groups used powders whereas all previous studies were performed on single crystals grown from a Bi-flux. Both experiments failed to observe a phase transition, except for R = Tm where Lonkai *et al* [13] observed the start of a transition, however without reaching the IP. Katsufuji *et al* measured until 1000 K for $YMnO_3$, synthesized in air, while our experiments show a transition at 1100 K. For R = Lu and Yb, neither Lonkai *et al* [13] nor Katsufuji *et al*

[12] measured at sufficiently high temperatures to observe a phase transition. For the smaller rare-earths the ferroelectric transition is expected to be higher than for R = Y [11]. Therefore, our work seems in agreement with previous literature, if one accepts that $YMnO_3$ grown in a Bi_2O_3 flux exhibits suppressed transition temperatures.

4. Conclusion

We provide experimental evidence for two high-temperature phase transitions in $YMnO_3$ using dilatometry, DTA and synchrotron x-ray powder diffraction. This is the first proof in one single experiment for the existence of an intermediate phase in $YMnO_3$. We describe these transitions at T_{C1} and T_{C2} as being probably second order in nature. Above T_{C2}, we confirm the existence of a paraelectric phase with $P6_3/mmc$ symmetry. We relate the higher transition temperatures of our crystal to the synthesis technique that we used. However, the nature of the intermediate phase remains to be investigated. Further experiments are in progress in order to give a full description of this system.

Acknowledgments

We thank M Brunelli, C V Colin, A J C Buurma and N Mufti for technical support during the experiment at ESRF. The work was supported by the Dutch National Science Foundation NWO by the breedtestrategieprogramma of the Materials Science Center, MSC$^+$. MP gratefully acknowledges the French Ministère de la Recherche et de la Technologie and the Délégation Régionale à la Recherche et à la Technologie, région Aquitaine, for financial support.

References

[1] Wang J, Neaton B, Zheng H, Nagarajan V, Ogale S B, Liu B, Viehland D, Vaithyanathan V, Schlom D G, Waghmare U V, Spaldin N A, Rabe K M, Wuttig M and Ramesh R 2003 *Science* **299** 1719
Kimura T, Goto T, Shintani H, Ishizaka K, Arima T and Tokura Y 2003 *Nature* **426** 55
Hur N, Park S, Sharma P A, Ahn J S, Guha S and Cheong S-W 2004 *Nature* **429** 392
[2] van Aken B, Palstra T T M, Filippetti A and Spaldin N A 2004 *Nat. Mater.* **3** 164
[3] Mostovoy M 2006 *Phys. Rev. Lett.* **96** 67601
[4] Katsura H, Nagaosa N and Balatsky A V 2005 *Phys. Rev. Lett.* **95** 57205
[5] Sergienko I A and Dagotto E 2006 *Phys. Rev.* B **73** 94434
[6] Huang Z J, Cao Y, Sun Y Y, Xue Y Y and Chu C W 1997 *Phys. Rev.* B **56** 2623
[7] Iliev M N and Lee H-G 1997 *Phys. Rev.* B **56** 2488
[8] Fiebig M, Lottermoser Th, Fröhlich D, Goltsev A V and Pisarev R V 2002 *Nature* **419** 818
[9] Lorenz B, Litvinchuk A P, Gospodinov M M and Chu C W 2004 *Phys. Rev. Lett.* **92** 87204
[10] Bertaut E F *et al* 1963 *C. R. Acad. Sci., Paris* **256** 1958
Bokov V A *et al* 1964 *Sov. Phys. Solid State* **5** 2646
Smolenskii G A *et al* 1964 *J. Appl. Phys.* **35** 915
Ismailzade I G and Kizhaev S A 1965 *Sov. Phys. Solid State* **70** 236
Peuzin J-C 1965 *C. R. Acad. Sci., Paris* **261** 2195–7
Coeure P *et al* 1966 *Proc. Int. Mtg on Ferroelectricity* vol 1, p 332
Lukaszewicz K and Karut-Kalicinska J 1974 *Ferroelectrics* **7** 81
[11] Abrahams S C *et al* 2001 *Acta Crystallogr.* B **57** 485
[12] Katsufuji T, Masaki M, Machida A, Moritomo M, Kato K, Nishibori E, Takata M, Sakata M, Ohoyama K, Kitazawa K and Takagi H 2002 *Phys. Rev.* B **66** 134434
[13] Lonkai T, Tomuta D G, Amann U, Ihringer J, Hendrikx R W A, Többens D M and Mydosh J A 2004 *Phys. Rev.* B **69** 134108
[14] Fennie C J and Rabe K M 2005 *Phys. Rev.* B **72** 100103
[15] Larson A C and von Dreele R B 1994 General Structure Analysis System GSAS *Los Alamos National Laboratory Report No.* LAUR 86-748 (unpublished)

[16] Sheldrick G M 2001 *SADABS Version 2. Multi-Scan Absorption Correction Program* (Germany: University of Göttingen)
[17] Bruker 2000 *SMART, SAINT, SADABS, XPREP and SHELXTL/NT. Area Detector Control and Integration Software. Smart Apex Software Reference Manuals.* (Madison, WI: Bruker Analytical X-ray Instruments)
[18] Lukaszewicz K *et al* 1974 *Ferroelectrics* **7** 81
[19] van Aken B, Meetsma A and Palstra T T M 2001 *Acta Crystallogr.* C **57** 230
[20] Yakel H L, Kochler W C, Bertaut F and Forrat E 1963 *Acta Crystallogr.* **16** 957
[21] Tolédano J-C and Tolédano P 1987 *The Landau Theory of Phase Transitions* (Singapore: World Scientific)
[22] Navard P and Haudin J M 1985 *J. Therm. Anal.* **30** 61
[23] Shannon R D and Prewitt C T 1970 *Acta Crystallogr.* B **26** 1046
Shannon R D and Prewitt C T 1969 *Acta Crystallogr.* B **25** 925
[24] Abrahams S C, Kurtz S K and Jamieson P B 1968 *Phys. Rev.* **172** 551